International Core Journal of Engineering Volume 6 Issue 9, 2020
ISSN: 2414-1895 DOI: 10.6919/ICJE.202009_6(9).0012

Highly Selective Bandpass Filter Based on SIR Slot and DGS

Wei Dai[1,a], Wusheng Ji[1,b], Siyu Zhao[1,c], Xiangwei Zhou[1,d]

[1]School of Electronic Engineering, Tianjin University of Technology and Education, Tianjin 300222, China.

[a]13820554343@163.com, [b]wshji1326@sohu.com, [c]ss15903365060@163.com, [d]15620033511@163.com

Abstract

A highly selective bandpass filter based on SIR (Stepped Impedance Resonator) grooves and DGS (Defected Ground Structure) is designed. The filter is composed of a microstrip-slot-microstrip multilayer structure. The top and bottom microstrip structures of the circuit realize interlayer coupling through the middle layer SIR-shaped groove and spiral DGS, and the coupling efficiency is high. The working frequency of the filter is 5.26-6.40GHz, the center frequency is 5.83GHz, and the fractional bandwidth is 19.6%; the filter insertion loss S21 is better than -1.5dB, the return loss S11 is better than -14.5dB, and the lower stopband is 4.3GHz and There is a transmission zero at the upper stopband at 7.2GHz, the stopband cut-off edge is relatively steep, and it has good in-band performance and frequency selectivity.

Keywords

Bandpass filter; Multi-layer interlayer coupling structure; SIR groove; Spiral DGS; high selectivity.

1. Introduction

As an important part of wireless communication systems, microwave filters are often used to distinguish signal frequencies, select useful signals, prevent noise interference, and improve equipment sensitivity. With the rapid development of wireless communication systems, the competition for spectrum resources has become increasingly fierce. In order to meet the requirements of large-capacity communication channels, the division of adjacent frequency spectrums is getting closer and closer, which puts forward higher requirements on the performance of the band-pass filter. In order to filter the adjacent frequency spectrum, the filter is required to have high selectivity.

There are many ways to improve filter selectivity. Reference [1] applies cross-coupling technology to add a new energy path between the resonant units of the filter or form a new path with the ground plane, which acts as an energy barrier and produces transmission zero points; Reference [2] The improved multimode resonator structure is used to improve the selectivity of the filter, but the passband bandwidth is narrow; the literature [3] uses a cascade suppression structure to improve the edge selectivity of the filter stopband, but the loss becomes larger, and the in-band S_{21} parameter performance Will be affected; literature [4] applies electromagnetic band gap structure (EBG, Electron Band Gap) or defective ground structure (DGS, Defected Ground Structure), by etching grooves on the ground plane, disturbing the distributed current on the ground plane, changing Transmission line characteristics, with band gap characteristics or slow wave characteristics; Literature [5] applies the application of changing the position of the input and output feeders to produce two transmission zeros on both sides of the passband; Literature [6] applies the load open stub structure to generate transmission zeros, But the influence of coupling type is not considered.

ISSN: 2414-1895 DOI: 10.6919/ICJE.202009_6(9).0012

In this paper, a multi-layer interlayer coupling structure is used, and the middle layer uses SIR-shaped grooves and DGS to design a highly selective band-pass filter. Compared with literature [3-4, 6], the band-pass filter has two transmission zero points, the in-band S-parameter performance is good, the pass-band selectivity is high, and it has practical value.

2. Filter Theory and Design

2.1 Circuit structure description

The designed filter is a multilayer circuit structure, which consists of two layers of dielectric substrates and three layers of metal boundaries. The top and bottom layers are both microstrip patch metal layers, the middle layer is a metal ground plane, and the top and bottom layers are coupled to transmit electromagnetic waves in the vertical direction through the middle layer. The top and bottom metal layers are all composed of 50Ω microstrip feeders, rectangular microstrip patches and half-wavelength SIR coupled with open ends; the middle layer is composed of a SIR-shaped slot loaded with open branches and spiral DGS on the left and right sides. The topology is shown in Figure 1. The top and bottom layers are oddly symmetrical about the middle layer.

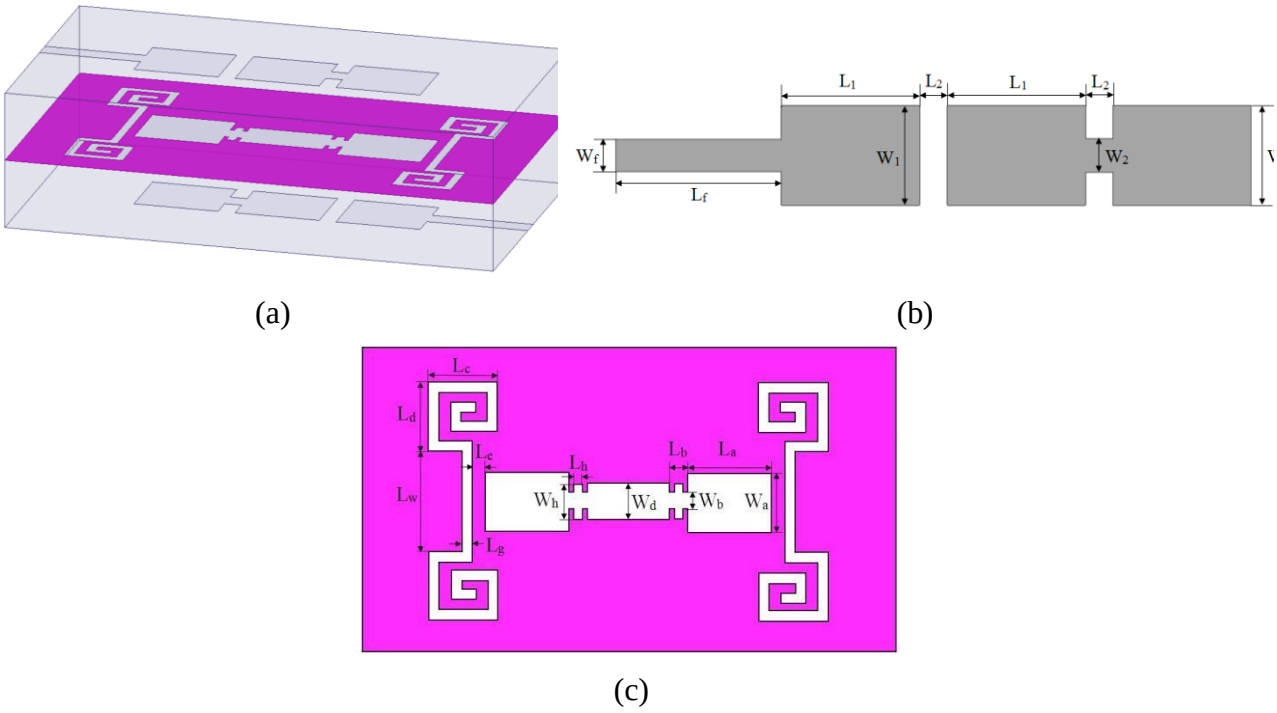

Fig. 1 Filter structure. (a) Three-dimensional structure diagram. (b) Top structure diagram. (c) Middle layer structure diagram.

In this paper, a 50Ω microstrip feeder line is laid on the top (bottom) metal layer to achieve 50Ω impedance matching in the application while taking into account factors such as withstand voltage, large power transmission and low loss; laying rectangular microstrip patches and open-ended coupling half-wavelength SIR are convenient In circuit processing, the resonance frequency can be controlled by changing the impedance ratio of the half-wavelength SIR [7]. An SIR groove is etched in the center of the metal ground plane of the middle layer, and the multi-layer interlayer coupling technology is used to realize the transmission of electromagnetic waves through the middle layer between the top and bottom layers. The circuit loss is small and the coupling efficiency is high. At the same time, the SIR groove is changed. Parameters such as impedance ratio and electrical length ratio can be adjusted to the frequency band range and passband bandwidth, which increases design flexibility; load spiral DGS at the left and right sides of the SIR groove, using the spiral DGS band

ISSN: 2414-1895 DOI: 10.6919/ICJE.202009_6(9).0012

rejection characteristics and double-pole attenuation Characteristic, produce transmission zero point, improve the frequency selectivity of band-pass filter; load open stubs at the SIR-shaped slot, play the role of impedance matching, and help improve the performance of S11.

2.2 The Influence of Multilayer Coupling Structure on S Parameters

The multi-layer interlayer coupling structure can make the transition of electromagnetic energy in the vertical direction occur between the dielectric layers. Because of its high coupling efficiency, it is mostly used in the design of multi-layer circuit structures. The multi-layer broadside coupling structure proposed in this paper is shown in Figure 2(a). The top layer and the bottom layer of the coupling structure are two rectangular microstrip patches of the same size, between which the coupling groove is etched in the center of the ground plane of the middle layer to realize the interlayer coupling in the vertical direction.

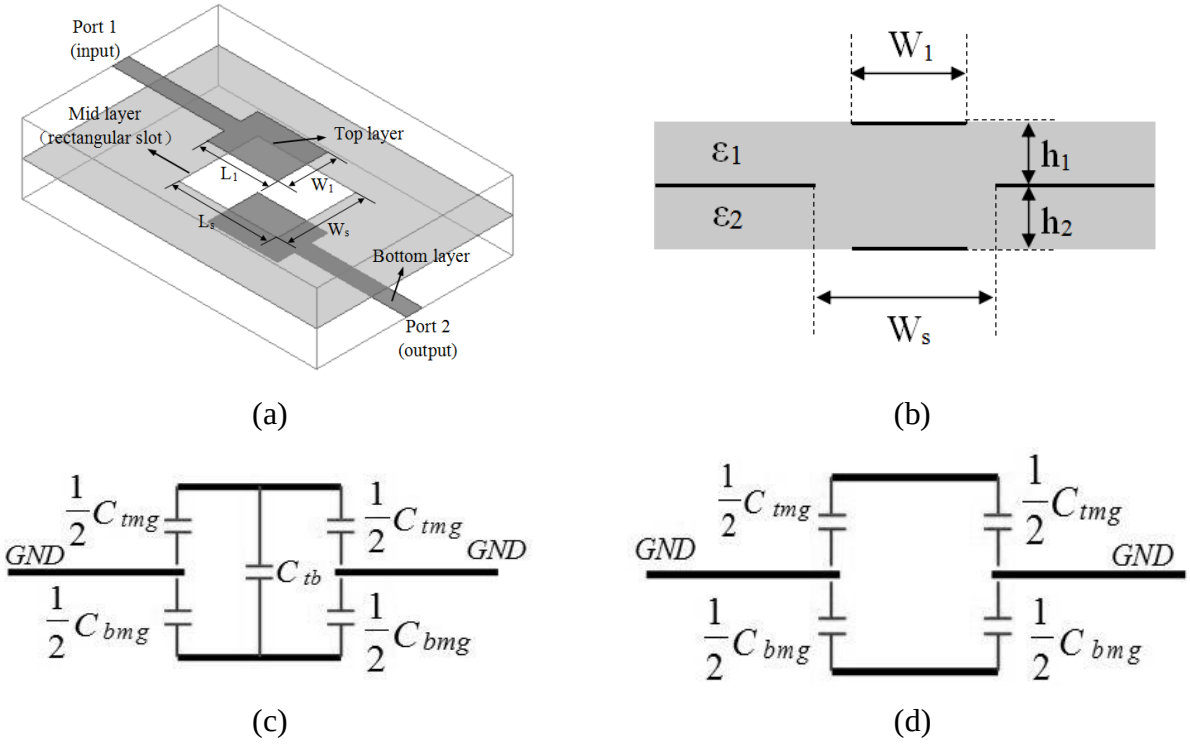

Fig. 2 Multilayer interlayer coupling structure. (a) Three-dimensional structure diagram. (b) Cross-sectional structure diagram. (c) Odd mode equivalent circuit. (d) Even mode equivalent circuit.

Suppose Port 1 and Port 2 are the input terminal and the output terminal, respectively. The length of the top and bottom rectangular microstrip patches is L_1 and the width is W_1, and the coupling groove length of the middle layer is L_s and the width is W_s.

According to the literature [8], the reflection coefficient S_{11} of the input port Port1 and the insertion loss S_{21} from the input port Port1 to the output port Port2 can be obtained:

$$S_{11} = \frac{1 - C^2\left(1 + \sin^2(\beta_{ef} L_1)\right)}{[\sqrt{1-C^2}\cos(\beta_{ef} L_1) + j\sin(\beta_{ef} L_1)]^2} \tag{1}$$

$$S_{21} = \frac{j2C^2\sqrt{1-C^2}\sin(\beta_{ef} L_1)}{[\sqrt{1-C^2}\cos(\beta_{ef} L_1) + j\sin(\beta_{ef} L_1)]^2} \tag{2}$$

ISSN: 2414-1895 DOI: 10.6919/ICJE.202009_6(9).0012

Among them, C is the coupling coefficient between the top and bottom patches. L_1 is the coupling length in the coupling structure, that is, the length of the top and bottom rectangular microstrip patches. β_{ef} is the equivalent phase constant. L_1 is approximately equal to the filter pass The quarter guide wavelength at the center frequency of the band.

Figure 2(b) is a cross-sectional schematic diagram of the broadside coupling structure. Figure 2(c) and Figure 2(d) are the even-odd-mode equivalent circuit diagrams of the multi-layer interlayer coupling structure. The microstrip-slot-line- The even and odd mode transmission characteristics of the micro-bandwidth edge coupling structure obtain the circuit coupling coefficient.

According to the literature [9], it can be concluded that the odd-mode coupling capacitor C_{to} between the top microstrip patch and the rectangular slot in the middle layer and the odd-mode coupling capacitor C_{bo} between the bottom microstrip patch and the rectangular slot in the middle layer satisfy the following relationship:

$$C_{to} = C_{tmg} + 2C_{tb}, \quad C_{bo} = C_{bmg} + 2C_{tb} \tag{3}$$

In the same way, the even mode coupling capacitor C_{te} between the top microstrip patch and the rectangular slot in the middle layer and the even mode coupling capacitor C_{be} between the bottom microstrip patch and the rectangular slot in the middle layer can be expressed as:

$$C_{te} = C_{tmg}, \; C_{be} = C_{bmg} \tag{4}$$

Among them, C_{tmg} and C_{bmg} are the coupling capacitances between the top and bottom microstrips and the rectangular grooves in the middle layer, respectively, and C_{tb} is the coupling capacitance between the top and bottom microstrips.

According to (3) and (4), the coupling coefficient between the top and bottom microstrip patches can be obtained as:

$$C = \sqrt{\frac{Z_{be}Z_{bo}}{Z_{te}Z_{to}}} \frac{Z_{te} - Z_{to}}{\sqrt{(Z_{be} + Z_{bo})(Z_{te} + Z_{to})}} \tag{5}$$

Among them, Z_{to} and Z_{bo} are the odd-mode equivalent impedances of the top and bottom microstrip patches, respectively, and Z_{te} and Z_{be} are the even-mode equivalent impedances of the top and bottom microstrip patches, respectively. According to literature [9], equation (5) It can be simplified further:

$$C = \frac{Z_{te} - Z_{to}}{\sqrt{(Z_{be} + Z_{bo})(Z_{te} + Z_{to})}} \tag{6}$$

When the upper and lower dielectric substrates are made of the same material and have the same thickness, that is, $\varepsilon_1=\varepsilon_2$, $h_1= h_2$, then $C_{to}=C_{bo}$, $C_{te}=C_{be}$, therefore, $Z_{to}=Z_{bo}$, $Z_{te}=Z_{be}$, then the top and bottom microstrips The coupling coefficient C between patches can be expressed as:

$$C = \frac{Z_{oe} - Z_{oo}}{Z_{oe} + Z_{oo}} \tag{7}$$

In formula (7), Z_{oo} and Z_{oe} are the odd-mode and even-mode impedances of the equivalent circuit, respectively. They can be calculated by the following formula[10]:

ISSN: 2414-1895 DOI: 10.6919/ICJE.202009_6(9).0012

$$Z_{oo} = \frac{60\pi}{\sqrt{\varepsilon_r}} \frac{K(k_1)}{K'(k_1)} \tag{8}$$

$$Z_{oe} = \frac{60\pi}{\sqrt{\varepsilon_r}} \frac{K(k_2)}{K'(k_2)} \tag{9}$$

Among them, $K(k)$ is the first type of elliptic integral, $K'(k) = K\sqrt{1-k^2}$, k_1, k_2 and the ratio of the elliptic function $\frac{K(k)}{K'(k)}$ can be calculated by the following formula[10]:

$$k_1 = \tanh(\pi W_1 / 4h) \tag{10}$$

$$k_2 = \left(\frac{\sinh^2(\pi W_s / 4h)}{\sinh^2(\pi W_s / 4h) + \cosh^2(\pi W_1 / 4h)} \right)^{\frac{1}{2}} \tag{11}$$

$$\frac{K(k)}{K'(k)} = \begin{cases} \frac{2}{\pi} \ln\left(2\sqrt{\frac{1+k}{1-k}} \right) & 0.707 \le k \le 1 \\ \frac{\pi}{2\ln\left(2\sqrt{\frac{1+\sqrt{1-k^2}}{1-\sqrt{1-k^2}}} \right)} & 0 \le k \le 0.707 \end{cases} \tag{12}$$

Among them, W_1 is the width of the top and bottom rectangular microstrip patches, W_s is the width of the coupling groove in the middle layer, and $h=h_1=h_2$ is the thickness of the dielectric substrate. By deriving formulas (1)-(12), it can be known that the even-odd-mode transmission impedance of the interlayer coupling structure can be adjusted by changing the length and width of the rectangular microstrip patch, which reflects the design flexibility of the structure.

2.3 The Influence of DGS on Passband Selectivity

In order to realize the high selectivity of the band-pass filter, a transmission zero is introduced at the upper and lower cut-off edges of the pass band. Generally speaking, the introduction of a multi-cascade structure can improve the selectivity of the upper and lower cut-off edges of the passband, but it will also increase the insertion loss S_{21} in the passband, which is detrimental to the improvement of filter performance. The introduction of DGS can improve the selectivity at the upper and lower cut-off edges of the filter passband without adding additional insertion loss.

DGS has a variety of circuit structures. The traditional DGS can produce a stop band, but the stop band is narrow and cannot suppress high-order harmonics; rectangular DGS can suppress high-order harmonics, but it is a single-pole low-pass stop band with only one Transmission zero point; although the dumbbell-shaped DGS has a simple structure and is easy to design, its band resistance characteristic is not good, the transition band of the frequency characteristic curve is not steep enough, and the equivalent inductance and equivalent capacitance are small, and the larger etching area can only Obtaining a smaller resonance frequency is not conducive to the miniaturization of microwave filters; spiral DGS is suitable for the miniaturization of microwave planar circuits. It can etch the squares on both sides of the transmission line into a spiral shape without occupying additional circuit area. , The circuit structure is more compact. At the same time, the spiral shape can effectively increase the equivalent inductance of the circuit, improve the stop-band characteristics of the circuit, and increase the passband selectivity of the filter.

The spiral DGS can be equivalent to a simple LC parallel resonant circuit, and its equivalent circuit diagram[11] is shown in Figure 3. The first resonant frequency and the second resonant frequency in Fig. 3 are the band-stop resonant frequencies at the upper and lower cut-off edges on both sides of the filter passband, respectively.

ISSN: 2414-1895 DOI: 10.6919/ICJE.202009_6(9).0012

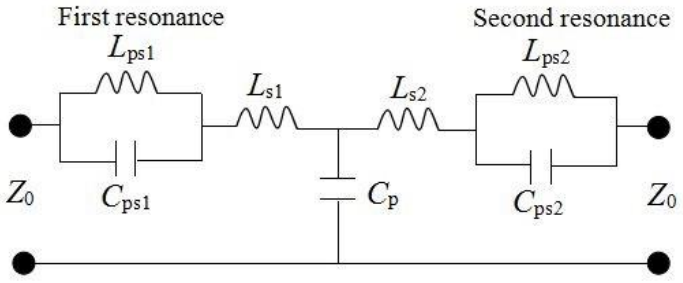

Fig. 3 Spiral DGS equivalent circuit model diagram.

The HFSS simulation software can be used to obtain the equivalent inductance L_{psi} and equivalent capacitance C_{psi} at the first and second resonant frequencies, and the equivalent inductance L_{si} at the transition frequency, and calculate by formulas (13)-(16)[11]. The first and second resonant frequencies of the spiral DGS are calculated.

$$f_T = \frac{1}{2\pi C_p X_{21}} \tag{13}$$

$$\Delta f_{3dB\_i} = \frac{1}{Z_0} \cdot \frac{1}{4\pi C_{psi}} \tag{14}$$

$$f_{0i} = \frac{1}{2\pi\sqrt{L_{psi} C_{psi}}} \tag{15}$$

$$f_{0i} = \frac{\sqrt{2\pi L_{si} f_T^2 - f_T (X_{ii} - X_{21})}}{\sqrt{2\pi L_{ps1}}} \tag{16}$$

Among them: f_{0i} (i=1,2) are the first and second resonance frequencies, Δf_{3dB_i} is the 3dB bandwidth at f_{01} and f_{02}, f_T is the transition frequency, and X_{11}, X_{22}, and X_{21} are the three Z parameters at f_T Imaginary part.

From formulas (13)-(16), the equivalent inductance of the spiral DGS is inversely proportional to the resonance frequency, that is, when the equivalent inductance is small, the resonance frequency is higher. To reduce the resonance frequency and keep the structure of the microstrip transmission line unchanged, it is only necessary to increase the geometric area of the spiral DGS. The increased area of the etched spiral shape can increase the equivalent inductance, thereby reducing the resonance frequency. The frequency response characteristic curve diagram of spiral DGS is shown as in Fig. 4.

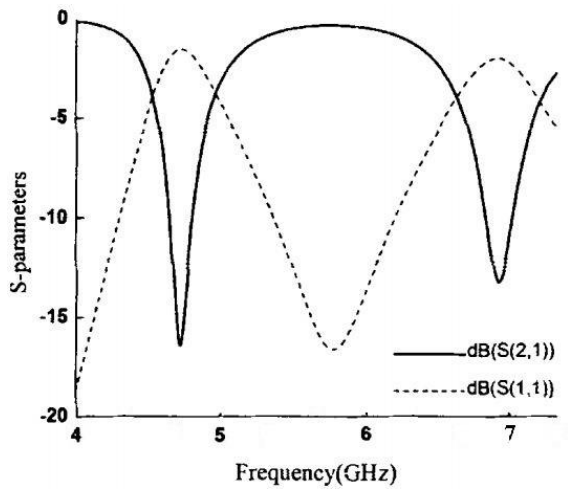

Fig. 4 Spiral DGS frequency response characteristic curve.

ISSN: 2414-1895 DOI: 10.6919/ICJE.202009_6(9).0012

It can be seen from Figure 4 that the spiral DGS has two attenuation poles, where S_{21} at 4.7 GHz and 7 GHz correspond to the first and second resonance frequency points in the equivalent circuit model of the spiral DGS in Figure 3, respectively. The double-pole band-stop characteristic of the spiral DGS is different from the single-pole band-stop characteristic of the traditional dumbbell-shaped structure. It is used in the design of bandpass filters to improve the frequency selectivity of the filter.

The filter is optimized by changing the design parameters of the spiral DGS, so that the resulting double-pole band-stop resonant frequency occurs exactly at the upper and lower cut-off edges on both sides of the pass band to obtain good pass-band and stop-band characteristics. From the optimization results, the spiral DGS parameters in this paper are shown in Table 1. Among them, L_c and L_d are the length and width of the spiral shape, and L_g and L_w are the length and width of the rectangular slit in the DGS.

Table 1 List of designed spiral DGS parameters

parameter	value	parameter	value
L_c	3.5mm	L_d	3.3mm
L_g	0.5mm	L_w	5.9mm

2.4 Simulation and Optimization

The filter circuit is further optimized, and open-circuit stub compensation is loaded at the SIR-shaped slot of the ground plane of the intermediate layer to improve the circuit matching performance. The optimized circuit parameters are as follows: the circuit uses two layers of RO4003 dielectric substrates with a thickness of 0.508mm, its dissipation factor is 0.0027, and the overall size is 29mm×16mm×1.016mm; the circuit top and bottom microstrip parameters L_f=6mm, L_1=5mm, L_2=1mm, W_f=1.15mm, W_1=4mm, W_2=1.2mm; the parameters of the SIR slot in the middle of the circuit are L_a=5mm, L_b=1mm, W_a=4mm, W_b=1.2 mm, W_d=2.6mm, the spiral DGS parameter is L_c=3.5mm, L_d=3.3mm, L_g=0.5mm, L_w=5.9mm, the spiral DGS and SIR groove gap is L_e=0.6mm, the open branch parameter is L_h=0.5mm, W_h=2.25mm.

The simulation result is shown in Figure 5. The working frequency of the filter is 5.26-6.40GHz, the center frequency of the passband is 5.83GHz, the fractional bandwidth is 19.6%, the insertion loss S_{21} in the passband is better than -1.5dB, and the return loss S_{11} is better than -14.5dB. There is a transmission zero at the lower stopband 4.3GHz and the upper stopband 7.2GHz, and the stopband cut-off edge is relatively steep, reflecting the good in-band performance and frequency selectivity of the filter. At the same time, the filter has the advantages of miniaturization, high performance, and good design flexibility, which is suitable for filter circuit design requirements.

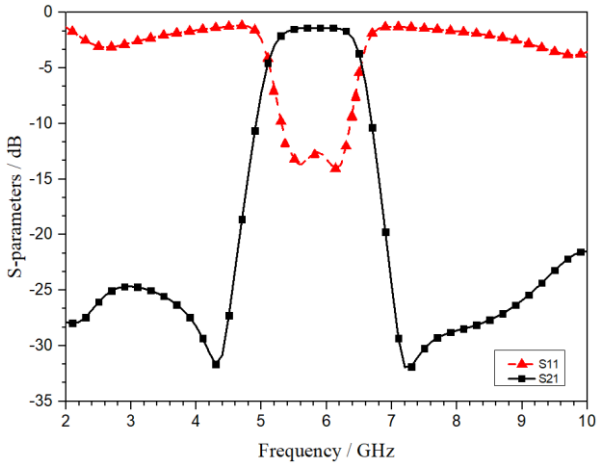

Fig. 5 Simulation results.

ISSN: 2414-1895 DOI: 10.6919/ICJE.202009_6(9).0012

3. Conclusion

In this paper, a high-selectivity band-pass filter is designed based on the multi-layer coupling structure and DGS. The working frequency of this filter is 5.26-6.40GHz, the center frequency is 5.83GHz, the fractional bandwidth is 19.6%, the insertion loss S_{21} is better than -1.5dB, and the return loss S_{11} is better than -14.5dB. The filter introduces a transmission zero at the upper and lower cut-off edges on both sides of the pass band to achieve high selectivity. The attenuation frequency characteristics on both sides of the pass band are adjusted by changing the spiral DGS parameters. In addition, in order to optimize circuit performance and achieve better circuit matching, an open stub is introduced into the SIR-shaped slot circuit to adjust the performance outside the passband. The filter is a multilayer circuit structure, which is conducive to circuit miniaturization and integration. This design still has some shortcomings, such as the 3dB fractional bandwidth at the passband is relatively narrow, and its broadbandization needs to be further studied in the future.

Acknowledgements

This work is supposed by the Natural Science Foundation of Tianjin, China (18JCYBJC16400), Graduate Innovation Foundation of Tianjin University of Technology and Education in 2020, China (YC20-3).

References

[1] Y.N. Mu, Z.W. Ma, D.M. Xu. A Novel Compact Interdigital Bandpass Filter Using Multilayer Cross-Coupled Folded Quarter-Wavelength Resonators[J], IEEE MICROWAVE AND WIRELESS COMPONENTS LETTERS,VOl. 15(2005) NO. 12, p.847-849.

[2] S.J. Sun, B. Wu, C.H. Liang. Novel dual-mode square ring microstrip bandpass filter[J], Journal of Xidian University, VOl. 41(2014) NO. 1, p.53-56.

[3] X.C. Ji, W.S Ji, L.Y. Feng, et al. Design of a Novel Multi-Layer Wideband Bandpass Filter with a Notched Band[J], Progress In Electromagnetics Research Letters, VOl. 82(2019), p.9–16.

[4] S. Zhang. Research on Structure and Performance of Miniature Planar Microwave Filter[M]. Shanghai: Shanghai University Press,2010.

[5] D.S. Cai, Z.Y. Lei, Y.J. Xie, et al. Design of Multi-band Out-of-band Zero-point Microstrip Bandpass Filter[J], Telecommunication Engineering, VOl. 5l(2011) No.11, p.89-93.

[6] C. Quenao, E. Rius.Narrow bandpass filters using dual behavior resonators based on stepped-impedance stubs and different length stubs[J]. IEEE Transactions on Microwave Theory and Techniques, VOl. 52(2004) No.3, p.1034-1044.

[7] M. Makimoto,S. Yamashita. Microwave resonator and filter in wireless communication[M]. Beijing: National Defense Industry Press, 2002.

[8] A.M. Abbosh. Planar Bandpass Filters for Ultra-Wideband Applications[J], IEEE TRANSACTIONS ON MICROWAVE THEORY AND TECHNIQUES, VOl. 55(2007) NO. 10, p.2262-2269.

[9] A.M. Abbosh, M. Bialkowski, S. Ibrahim. Ultra-wideband bandpass filters using broadside-coupled microstrip-coplanar waveguide[J], IET Microwaves Antennas & Propagation,VOl. 5(2011) NO.7, p.764–770.

[10] A.M. Abbosh, M. Bialkowski. Design of Compact Directional Couplers for UWB Applications[J], IEEE TRANSACTIONS ON MICROWAVE THEORY AND TECHNIQUES, VOl. 55(2007) NO. 2, p.189–194.

[11] H. Chen. Modern radio frequency radio frequency microwave planar circuit[M]. Electronic Industry Press, 2016.